A SENSOR INVARIANT ATMOSPHERIC CORRECTION METHOD FOR SATELLITE IMAGES

Feng Yin[1], *J Gómez-Dans*[1,2], *P Lewis*[1,2]

[1]Dept. of Geography, University College London, UK
[2] National Centre for Earth Observation (NCEO), UK
2

ABSTRACT

We propose a data fusion method for atmospheric correction of satellite images, with an initial attempt to include the uncertainty information from different data sources. It takes advantage of the high temporal resolution of MODIS observations to get specral BRDF description of the earth surface as prior information for the land surface, uses the ECMWF CAMS Near-real-time as the prior information on atmospheric composition. It ensures the correction is consistent cross different satellites image tiles and even cross different sensors. The validations of retrieve AOT against AERONET sites are also show high correlation at around 0.9, with a RMSE of about 0.02.

1. INTRODUCTION

Data captured by optical sensors on board satellites is affected by atmospheric effects (such as scattering and absorption of photons by gases and particles within the atmosphere), as well as atmosphere-surface effects. It is important to compensate for these effects in order to provide observations that only pertain to the state of the land surface. To this end, a number of atmospheric correction schemes have been developed. Some of these methods are empirical, whereby reference areas (usually open water or very dark vegetation) are assumed to have a reflectance of zero. The measured reflectance is then assumed to come from atmospheric effects, which are then subtracted to from all pixels. A major shortcoming of this approach is the assumption of spatial stationarity of the atmospheric effects, and the reliance on these so-called dark objects, which might be few and far between. More sophisticated methods, such as the MODIS dark dense vegetation (DDV) method [1], makes a pragmatic use of an empirical relationship between shortwave infrared (SWIR) reflectance at 2100 nm and blue and red reflectance. This coupling is then used within a look up table to invert the 6S model[2] and retrieve atmospheric composition parameters. Recently, new methods have started exploiting the relatively slow change of land surface reflectance in comparison to the very fast variation of atmospheric composition. [3] developed an algorithm based on this concept and showed a good agreement to the AERONET measurements. A more sophisticated method is developed by [4] for the atmospheric correction of MODIS TOA reflectance, which takes the angular effects into account and uses the BRF of surface within a shorter time interval. [5] used empirical linear relationship between spectral bands to infer the surface reflectance at visible bands, and a temporal constrain is also used under the concept of relative invariant surface reflectance mentioned above. The performance of these algoirthms inevitably degrades in situations where observations of the surface are few or large gaps between acquisitions are present.

In this contribution, we propose a new method that builds up on the previous approaches (particulary

We propose a new method taking advantage of the high temporal resolution of MODIS observations to get BRDF description of the earth surface as the *prior* information of the earth surface property, using the ECMWF CAMS Near-real-time as the prior information of the atmospheric sates, to get an optimal estimation of the atmospheric parameter. The atmospheric radiative transfer function used is the 6S and emulation method using GP is also used for fast implementation and propagation of uncertainty in the non-linear radiative transfer function [6].

2. DATA AND PRE-PROCESSING

2.1. Sentinel 2 TOA reflectance

As a heritage program of LANDSAT and SPOT, S2 (s) is mounted with 10m, 20m and 60m spatial resolution Multi-Spectral Instrument (MSI), having 13 spectral bands ranging from 443 *nm* to 2190 *nm*. With narrower bandwidth compared to LANDSAT and SPOT, e.g. band 8a at 865 nm has a 20 nm bandwidth, S2 bands are less contaminated by atmospheric influences, especially in water vapour absorption bands. Band 1 (443 *nm*) is specified for accurate aerosol correction, and band 10 (1375 *nm*) is for the detection of cirrus clouds that potentially affect the reflectance values. Sentinel-2 L1C products are radiometrically and geometrically corrected TOA reflectance, including the ortho-rectification and spatial registration on Military Grid Reference System (MGRS) system with sub-pixel accuracy.

2.2. MODIS MCD43 BRDF products

500 m MODIS collection 6 BRDF/Albedo products are produced daily, composting of 16 days surface reflectance anisotropy measurements from both Tera and Aqua platforms [7], which is a compromise of sufficient angular samples and the surface is assumed to be static at this limited period [8]. A kernel-driven linear BRDF model, Ross-Thick/Li- Sparse-Reciprocal (RTLSR) is deployed to estimate surface BRDF, using a constant parameter for isotropic scattering and two kernels, the RossThick and LiSparse-Reciprocal [9], for the

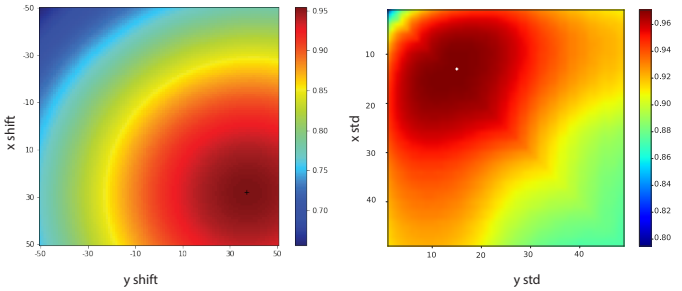

Fig. 1. The error surface of shifts and standard deviations in x and y direction

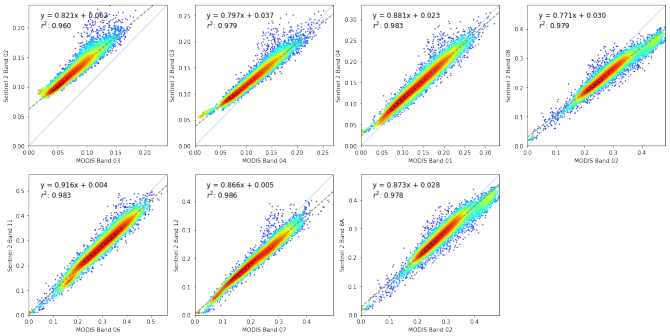

Fig. 2. The linear regression between Sentinel-2 and MODIS bands after applying PSF model

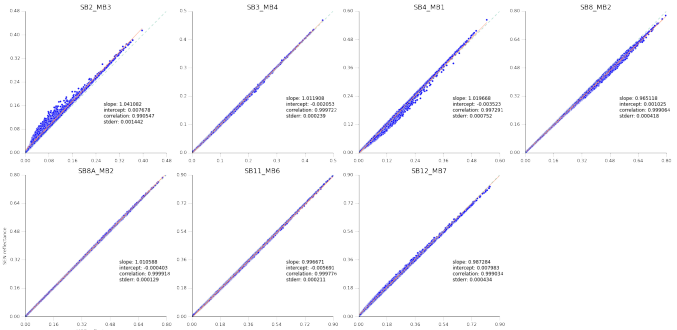

Fig. 3. The linear regression results of Sentinel-2 and MODIS convolved with the relative response functions

volumetric and geometric scattering respectively, which is given by:

$$\rho(\lambda_M, \Omega, \Omega') = f_{iso}(\lambda_M) + f_{vol}(\lambda_M) K_{vol}(\Omega, \Omega') + f_{geo}(\lambda_M) K_{geo}(\Omega, \Omega') \quad (1)$$

where $\rho(\lambda_M, \Omega, \Omega')$ is MODIS reflectance at wavelength $\rho(\lambda_M)$, viewing vector Ω and solar illumination vector Ω', in which two angular vectors contain both the zenith and azimuth angles. $K_{vol}(\Omega, \Omega')$ is the volumetric scattering kernel and $K_{geo}(\Omega, \Omega')$ is the geometric scattering kernel.

Sentinel-2 sensing geometry is used to compute the kernel values $k_{geo}\left(\Omega, \Omega^{'}\right)$ and $k_{vol}\left(\Omega, \Omega^{'}\right)$. f_{iso}, f_{vol} and f_{geo} from MCD43A1 are used with those kernel values to compute the simulated surface reflectance values at MODIS spatial and spectral resolution while in the Sentinel-2 viewing and solar illumination angle.

3. PSF MODELLING

Due to the big differences in the spatial resolution between the MODIS (500 m) and Sentinel-2 (10 m), only the MODIS PSF is considered in the implementation. Equivalent PSF for MODIS is estimated by maximising the correlation between the Sentinel-2 band 12/11 TOA reflectance convolved with MODIS PSF with the MODIS MCD43 BRDF products simulated surface reflectance at Sentinel viewsing angles. The reason for using Sentinel-2 band 12 or 11 is that atmosphere tends to have samller effects on those 2 SWIF bands compared to the shorter wavelength bands, especially aersol effects. The error surfaces of PSF modelling are first illustrated with the shifts and standard deviations in x and y direction individually in Figure 1.

Since the standard deviations in x and y direction is mainly controlling the extend of PSF model, which should be around triple the size of 500 m one MODIS pixel according to the ideal PSF shape of MODIS, and they do not vary that much in different area in our solved results. Additionally, the error surface also showed that the changes of correlation with the standard deviation is less significant compared to that with shifts. Thus, fixed standard deviations in x and y direction are used and only the shifts in x and y direction are solved, which also saves a lot of time for the solving of PSF model parameters and an example of correlation between MODIS and Sentinel-2 bands in Figure 2.

4. SPECTRAL MAPPING

In the work of GlobAlbedo [10], linear model is used for the transform of albedo from narrow bands to broad bands. We extend this idea to map MODIS bands and Sentinel-2 bands by the using of linear model. Spectral data from ESA ADAM study are used to simulate the MODIS and Sentinel-2 spectra by applying the relative spectral response function of them and then inversion of two matrix give us the spectral mapping matrix, which then can be used to convert one sensor measurements to another. The uncertainty information is also estimated in this process. For easy implementation, only the closest MODIS and Sentinel-2 bands are used for the retrieval of spectral transfer between MODIS and Sentinel-2. In that way, only two term, *i.e.*, slope and intercept, are used for the transformation between MODIS and Sentinel-2 bands (Figure 3).

5. SOLVING ATMOSPHERIC PARAMETERS

After applying the PSF model and spectral mapping function to the Sentinel-2 TOA reflectance and MODIS simulated surface reflectance respectively, then we have TOA and BOA reflectance at Sentinel-2 spectral bands and at MODIS spatial resolution. By coupling the atmospheric radiative transfer models, such as MOTRAN or 6S (used in this method), with control variables, viewing angles, sun illumination angles and elevation and priors values for AOT, TCWV and TCO_3 from ECMWF, we can get the *posterior* estima-

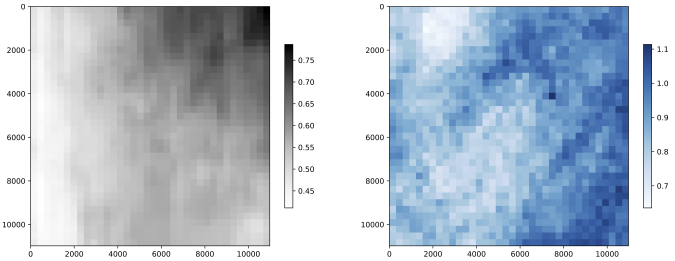

Fig. 4. A solved AOT(left) and TCWV(right) map, which shows a slowly changing of AOT from bottom left corner to the up right corner

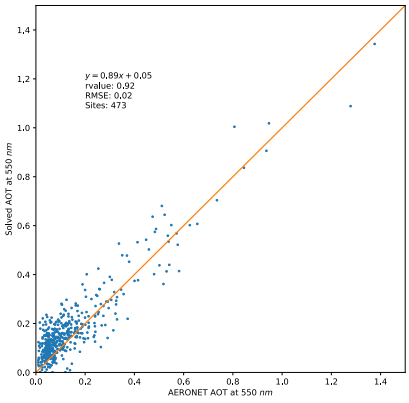

Fig. 5. Validation against AERONET sites

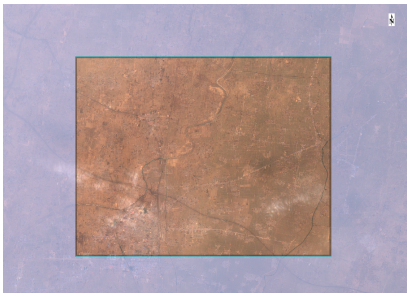

Fig. 6. A demonstration of correction over North China plain, where it has a very high aerosol loading and with few dark dense vegetation, and this method still shows a relative good correction.

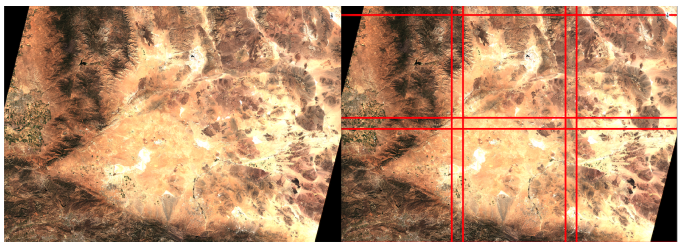

Fig. 7. A MOSAIC image composed of 6 Sentinel 2 tiles, and the red lines on the right are the borders of individual Sentinel 2 tile. From this image, this method shows a consistent correction for neighbour tiles.

tion for AOT, TCWV and TCO_3. In the solving process, we also considering the uncertainty information for the *priors* and observations, *i.e.* MODIS simulated surface reflectance, and an extra spatial smoothing model is also used with an uncertainty is also used under the fact that atmospheric parameters varying slowly spatially. Thus, Three cost functions are built for the optimisation of atmospheric parameters under the assumption that Gaussian distribution for all the aspects this system:

$$J_{obs}(x) = 0.5(R - H(x))^\top C_{obs}^{-1}(R - H(x)) \text{ Observations}$$
$$J_{prior}(x) = 0.5(x - x_{prior})^\top C_{prior}^{-1}(x - x_{prior}) \text{ Prior}$$
$$J_{smooth}(x) = 0.5\gamma^2 x^\top (D^\top D)x \text{ Smooth}$$

Where R is PSF convolved TOA reflectance, x MODIS simulated surface reflectance, H observation operator, *i.e.* 6S radiative transfer model, C is the covariance matrix for observation and prior, γ is the smoothness term and D is the differential operator. Then we can calculate the derivative of each cost function as well.

Under the Bayesian context, the maximum likelihood estimate of the state variables x is by minimising the sum of all the cost functions, and the derivative of each cost function is summed up for fast searching of *posterior* estimations of state variables x, and here refers to atmospheric parameters.

GP emulation method is used to emulate the radiative transfer model, and we use a Lambertian assumption for the earth surface with no angular effects at current version. Emulators for all the Sentinel-2 bands are created, with inputs of sun and view angles, elevation and atmospheric parameters. Another benefits of using emulators is that the uncertainty is analytically propagated and partial derivatives of all parameters are estimated at the same time, which make it possible to have a fast and accurate implementation of radiative transfer model in the solving of atmospheric parameters.

An example of solved AOT and TCWV is given in Figure 4, and the validation against the AERONET measurements, which is interpolated to AOT at 550 nm, is shown in Figure 5. There is a bias in the regression results between the solved results and the AERONET measurements, which is possible come from a continental aerosol model is used for all sites which would affect the solved aerosol value [11]. According to [12], the same aerosol model is used for the retrieval and correction and self compensating error will further reduce the bias reported in comparison with AERONET measurements in the correction results.

6. ATMOSPHERIC CORRECTION

Using the solved atmospheric parameters, atmospheric correction can be done with emulators used in the solving process. In the current version, we do not correct for the adjacent effects and terrain effects, and we assume an isotropic land surface and do not correct for the BRDF effects as well. Some correction example correction results in Figure 6 and Figure 7, and a simple comparison with

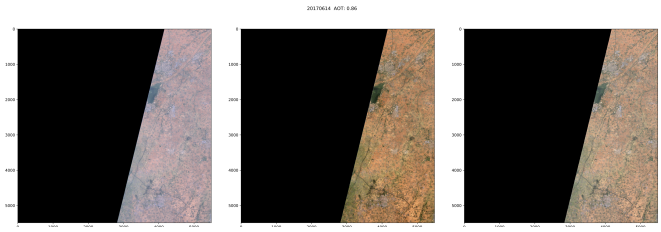

Fig. 8. Corrected surface reflectance RGB image in comparison with Sen2Cor correted results. From left to rgiht are TOA reflectance, corrected with this method and Sen2Cor corrected reflectance. The mean AOT of 0.86 is shown as an averaged aerosol loading across this tile.

Sen2Cor results in Figure 8.

7. CONCLUSION

A new atmospheric correction method is proposed in this contribution, which uses all the available information as *prior* under Bayesian context, and it shows promising results in the retrieved atmospheric parameters and the correction results. That demonstrates an atmospheric correction method like this is able to incorporate all the available information and provide reasonable atmospheric corrections of satellite images for various sensors, leading to a sensor invariant correction of satellite images. More importantly, this method is also able to propagate uncertainty information cross the whole system.

Acknowledgements

The authors would like to acknowledge financial support from the European Unions Horizon 2020 research and innovation programme under grant agreement No 687320.

8. REFERENCES

[1] Y. J. Kaufman, D. Tanré, L. A. Remer, E. F. Vermote, A. Chu, and B. N. Holben, "Operational remote sensing of tropospheric aerosol over land from EOS moderate resolution imaging spectroradiometer," *Journal of Geophysical Research: Atmospheres*, vol. 102, no. D14, pp. 17051–17067, 7 1997.

[2] E.F. Vermote, D. Tanre, J.L. Deuze, M. Herman, and J.-J. Morcette, "Second simulation of the satellite signal in the solar spectrum, 6s: an overview," *IEEE Transactions on Geoscience and Remote Sensing*, vol. 35, no. 3, pp. 675–686, 3 1997.

[3] Shunlin Liang, Bo Zhong, and Hongliang Fang, "Improved estimation of aerosol optical depth from MODIS imagery over land surfaces," *Remote Sensing of Environment*, vol. 104, no. 4, pp. 416–425, 10 2006.

[4] Alexei Lyapustin, John Martonchik, Yujie Wang, Istvan Laszlo, and Sergey Korkin, "Multiangle implementation of atmospheric correction (MAIAC): 1. radiative transfer basis and look-up tables," *Journal of Geophysical Research*, vol. 116, no. D3, 2 2011.

[5] Olivier Hagolle, Mireille Huc, David Pascual, and Gerard Dedieu, "A multi-temporal and multi-spectral method to estimate aerosol optical thickness over land, for the atmospheric correction of FormoSat-2, LandSat, VENS and sentinel-2 images," *Remote Sensing*, vol. 7, no. 3, pp. 2668–2691, 3 2015.

[6] José Luis Gómez-Dans, Philip Edward Lewis, and Mathias Disney, "Efficient emulation of radiative transfer codes using gaussian processes and application to land surface parameter inferences," *Remote Sensing*, vol. 8, no. 2, pp. 119, 2016.

[7] Crystal B Schaaf, Feng Gao, Alan H Strahler, Wolfgang Lucht, Xiaowen Li, Trevor Tsang, Nicholas C Strugnell, Xiaoyang Zhang, Yufang Jin, Jan-Peter Muller, Philip Lewis, Michael Barnsley, Paul Hobson, Mathias Disney, Gareth Roberts, Michael Dunderdale, Christopher Doll, Robert P d'Entremont, Baoxin Hu, Shunlin Liang, Jeffrey L Privette, and David Roy, "First operational brdf, albedo nadir reflectance products from modis," *Remote sensing of Environment*, vol. 83, no. 1, pp. 135–148, 2002.

[8] W. Wanner, Xiaowen Li, and A.H. Strahler, "A new class of geometric-optical semiempirical kernels for global BRDF and albedo modeling," 1995.

[9] X. Li and A.H. Strahler, "Geometric-optical bidirectional reflectance modeling of the discrete crown vegetation canopy: effect of crown shape and mutual shadowing," *IEEE Transactions on Geoscience and Remote Sensing*, vol. 30, no. 2, pp. 276–292, mar 1992.

[10] P Lewis, L Guanter, G Lopez, JP Muller, N Shane, J Fisher, P North, A Heckel, O Danne, and C Brockmann, "Globalbedo algorithm theoretical basis document v3. 1," 2012.

[11] Bastien Rouquié, Olivier Hagolle, François-Marie Bréon, Olivier Boucher, Camille Desjardins, and Samuel Rémy, "Using copernicus atmosphere monitoring service products to constrain the aerosol type in the atmospheric correction processor MAJA," *Remote Sensing*, vol. 9, no. 12, pp. 1230, nov 2017.

[12] EF Vermote and A Vermeulen, "Atmospheric correction algorithm: spectral reflectances (mod09)," *ATBD version*, vol. 4, 1999.